crystals

MDPI

Article

Chiral Photoresponsive Liquid Crystalline Materials Derived from Cyanoazobenzene Central Core: Effect of UV Light Illumination on Mesomorphic Behavior

Anna Poryvai [1], Alexej Bubnov [2] and Michal Kohout [1,*]

[1] Department of Organic Chemistry, University of Chemistry and Technology Prague, Technická 5, 166 28 Prague, Czech Republic; poryvaia@vscht.cz

[2] Institute of Physics of the Czech Academy of Sciences, Na Slovance 1999/2, 182 21 Prague, Czech Republic; bubnov@fzu.cz

* Correspondence: michal.kohout@vscht.cz; Tel.: +420-22044-4118

Received: 2 November 2020; Accepted: 15 December 2020; Published: 21 December 2020

Abstract: One of the most frequently utilized liquid crystalline (LC) materials is a rod-like (calamitic) compound 4-cyano-4′-pentylbiphenyl (5-CB). The main objective of this work is to enhance its functionality by introducing a photoresponsive diazenyl spacer in the aromatic core and replace the non-chiral pentyl chain with various chiral alkyl carboxylate units. The mesomorphic properties of the prepared materials have been studied using polarizing optical microscopy and differential scanning calorimetry. It has been found that materials with an extended aromatic system possess the liquid crystalline behavior. The studied LC materials have shown mesophases at lower temperatures than previously reported analogous substances. Furthermore, one of them exhibits a chiral orthogonal frustrated twist grain boundary smectic phase, which has not been previously observed for this structural type of materials. We also investigated photoresponse of the mesophases under illumination with UV-light (365 nm) using a polarizing optical microscope. A non-conventional photoresponse of the prepared materials in a crystalline phase is presented and discussed.

Keywords: photoresponsive chiral liquid crystals; photoresponse; azobenzene; cyanoazobenzene; 5-CB; twist grain boundary phase

1. Introduction

Due to their extraordinary ability to form various self-organized supramolecular structures between solid and liquid states (mesophases) [1], thermotropic liquid crystals (LCs) are widely used as smart organic materials. Since in a mesophase, the LCs combine the fluidity of liquids and ordering of crystals, their structure, and the optical properties, can be easily tuned by an applied electric field or by a temperature change. Tunability of mesophases using light requires the introduction of a photoresponsive moiety into the structure of LC molecules. Illumination with light then induces changes in geometry of LC molecules, which leads to the isothermic changes in the structure of formed mesophases, eventually to supercooling of a phase transition [2]. During last decade, the photoresponsive materials have received considerable attention due to their possible application in data storage systems [3], tunable photonic devices [4,5], artificial muscles [6,7], and other smart applications [8–10].

General structure of calamitic LC molecules can be described as a combination of relatively rigid parts, typically aromatic cores with/without linking groups, with flexible parts, usually represented by terminal alkyl chains [11]. The introduction of a chiral center in the flexible alkyl chain gives rise to chiral

liquid crystals, whose mesophases can be easily modulated by external electric field, and thus, represent a class of materials with broad application potential in electro-optical devices. One of the best known and most widely used achiral LC material is a calamitic (rod-like) 4-cyano-4′-pentylbiphenyl (**5-CB**), which forms a nematic mesophase (N) at room temperature [12] and, hence, attracts considerable attention due to its potential applicability. A chiral homologue of **5-CB** (**$C_2H_5CH(CH_3)C_2H_4$-CB**) was also prepared and studied [13]. Generally, the structural motif of **5-CB** has been successfully implemented in a variety of LCs; different types of symmetrical [14,15] or non-symmetrical dimeric LCs [16,17], metal containing LCs [18,19] as well as ligands for stabilization of nanoparticles in LC hosts [20,21] have been designed and synthesized.

In order to tune mesomorphic properties of **5-CB**, various structural modification have been employed (Figure 1). Among them, replacing the alkyl terminal chain in **CB**-based materials with an alkoxy terminal chain provided **OCB** materials, such as **6-OCB** and **12-OCB**, or the introduction of the ester group in **8-COOCB** [22,23]. Moreover, in this case, the substitution in the alkyl chain provided chiral materials **$C_2H_5CH(CH_3)C_2H_4$-OCB, $H_{17}C_8$OPh-CH(CH_3)-COOCB**), which exhibited chiral nematic phase at very low temperatures [13,24,25]. Furthermore, modifications in the central core involving substitution of one benzene core for cyclohexane [26,27] or a heterocyclic core [28,29], the introduction of lateral substituents [30–34], as well as the introduction of a linker between the aromatic units (e.g., the photoresponsive diazenyl group in **7-CAB**, **7-OCAB**, **9-OC_6H_4-COO-CAB**, **6-OC_6H_4-COO-CAB**) were described [35–39]. The diazenyl group is a chemically stable photoswitchable moiety, which undergoes reversible *E*/*Z*-isomerization under illumination, thus, providing the possibility to tune the molecular organization within mesophases. To date, only a single chiral photosensitive material based on 4′-hydroxy-4-cyanoazobenzene (OCAB) has been described [40].

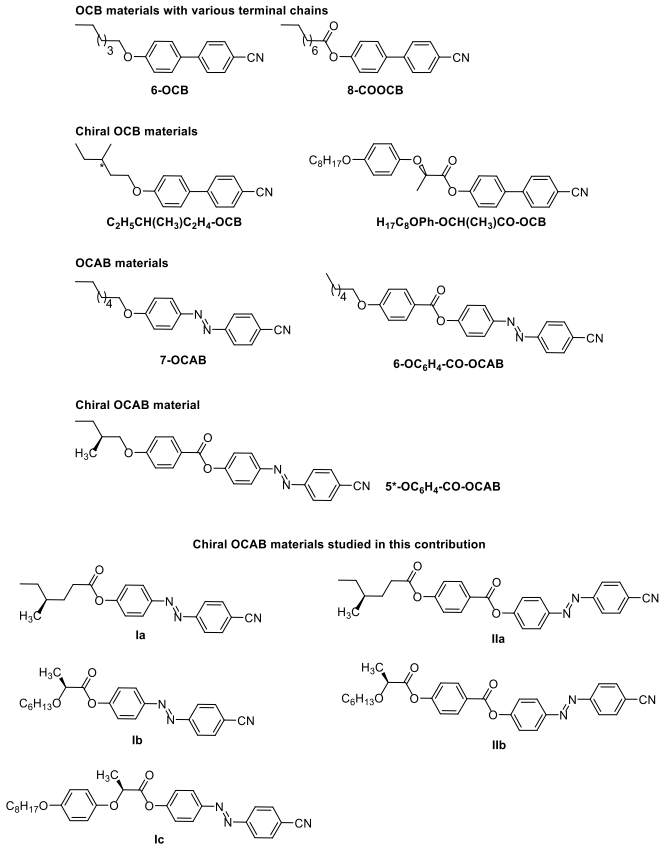

Figure 1. Structures of the materials derived from **5-CB** and materials studied here. Chiral centers are indicated by asterisk or by defined position one of the substituents. References to the depicted compounds are provided later in the text.

Hereby we designed, synthesized, and studied the mesomorphic properties of novel representatives of CAB-based chiral photosensitive LCs. In order to study the structure–property relationships, we designed five materials, which differed in chiral units attached to the central core through an ester group. To our best knowledge, the photoresponse of such chiral OCAB-based materials has not been studied yet.

2. Materials and Methods

2.1. Design and Synthesis of the Materials

The design of the target chiral photoresponsive materials **Ia-c** and **IIa-b** was inspired by the basic structure of **5-CB**, which was modified in two different ways. Firstly, the biphenyl core was extended using the photoresponsive diazenyl N=N linker (Figure 2, green). Secondly, a non-chiral elongating alkyl chain (C_5H_{11} in **5-CB**) was replaced by a chiral unit R (Figure 2, blue), which was attached to the central core through an ester linking unit (Figure 2, red). In order to investigate structure–property relationships, various chiral units were connected to the central core. Materials **Ia,b** contained lactic or 4-methylhexanoic acid-based chiral units. For the material **Ic**, the chiral part was extended by an aromatic core, in order to investigate the effect of moving the chiral unit close to the center of the molecule. Materials **II** then contained the rigid core elongated with 4-hydroxybenzoic acid. Therefore, the system of connected aromatic rings was extended from two (for materials **Ia,b**) to three (for materials **Ic** and **IIa,b**). A compound **IIc** has not been synthesized due to expected high transition temperatures imposed by four aromatic rings in such a structure.

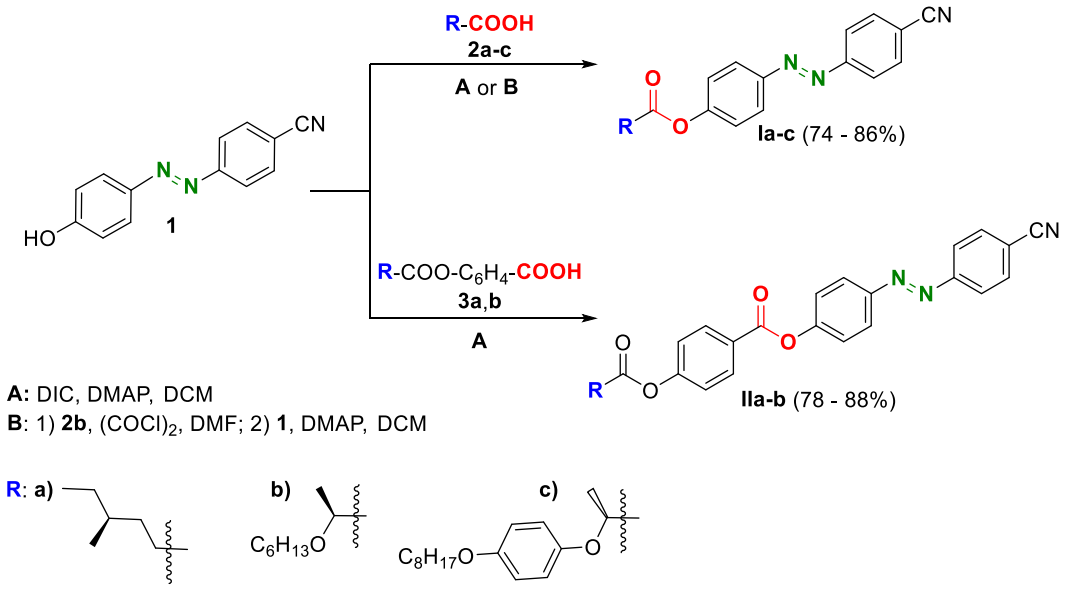

Figure 2. Synthesis of the target materials **Ia-c** and **IIa-b**. Two synthetic methods, A and B, were used. Chiral units, R, are marked in blue and depicted at the bottom of the figure.

Designed materials were synthesized in high yields by connection of the known building blocks: phenol **1** [41] with acids **2a-c** [13,42,43] or acids **3a,b** [44–46] using DIC-mediated acylation reaction (**A**) or by acylation using corresponding acid chloride in the presence of DMAP (**B**) (Figure 2). The method **B** was used for direct acylation of the central core **1** with (*S*)-2-octyloxypropanoic acid chloride because of potential racemization of the chiral acid in the DIC-mediated esterification reaction [46–48].

2.2. Synthesis and Characterization

All commercially available reagents were purchased from Merck (Darmstadt, Germany) and TCI Chemicals Europe (Zwijndrecht, Belgium) and used without further purification.

Chiral acids: (*S*)-4-methylhexanoic acid **2a** [49]; (*S*)-2-(hexyloxy)propanoic acid **2b** [43]; (*R*)-2-[4-(octyloxy)phenoxy]propanoic acid **2c** [23]; (*S*)-4-(4-methylhexanoyloxy)benzoic acid **3a** [44] and (*S*)-4-(2-hexyloxypropanoyloxy)benzoic acid **3b** [44–46] were prepared in our laboratory according to known procedures and their analytical data corresponded to that described in the literature. Dry dichloromethane (DCM) was taken from a solvent purification system PureSolv MD7 (Amesbury, MA, USA). Kieselgel 60–100 μm (Merck, Darmstadt, Germany) silica was used for column chromatography.

The structure of final products was confirmed by IR spectroscopy, NMR spectroscopy, and mass spectrometry. IR spectra were recorded using Thermo Scientific™ Nicolet™ iS™10 FT-IR Spectrometer (Thermo Fischer Scientific, Waltham, MA, USA) on KBr discs. ^{1}H and ^{13}C NMR spectra were acquired on Agilent 400-MR DDR2 spectrometer (Agilent Technologies, Santa Clara, CA, USA), chemical shifts (δ) are given in ppm, and spin–spin coupling constants (*J*) in Hz. Deuterated chloroform ($CDCl_3$) was used as a solvent. The residual non-deuterated solvent peak was used as an internal standard for ^{1}H and ^{13}C NMR spectra. Multiplicity of recorded peaks is described using following abbreviations: d—doublet, t—triplet, q—quartet, m—multiplet. The exact mass of the target compounds was obtained with high-resolution mass spectrometer LTQ Orbitrap Velos (Thermo Fischer Scientific, Waltham, MA, USA).

Two methods of acylation **A**, **B** were used to prepare target molecules. Method **A** was used for the synthesis of all target materials (except for the compound **Ib**) and, therefore, it is described as a general method.

General method **A**. The solution of an alcohol 1 (1.1 mmol) in DCM (25 mL) was added dropwise to a solution of a corresponding acid (1.0 mmol) with N,N-diisopropylcarbodiimide (DIC) (1.1 mmol) and a catalytic amount of *N*,*N*-dimethylaminopyridine (DMAP) (1.0 mmol) in DCM (50 mL) in the inert atmosphere of argon. The reaction mixture was stirred for 2 h and then the reaction was quenched with water. Layers were separated and the aqueous layer was extracted with toluene (2 × 20 mL). The combined organic solution was washed with brine (10 mL) and dried with anhydrous magnesium sulfate. The solvent was evaporated under reduced pressure and the crude orange product was purified by column chromatography (eluent: chloroform) and crystallization from ethanol (3 times).

(S)-4-[(4-Cyanophenyl)diazenyl]phenyl 4-methylhexanoate (Ia)

The material **Ia** was prepared according to the method **A** in 74% (118 mg) yield as orange crystals, m.p. 92–93 °C.

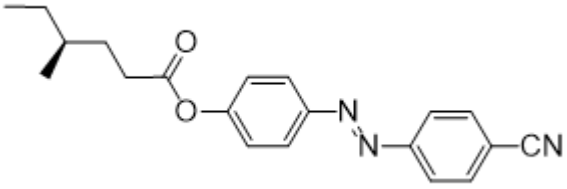

^{1}H NMR (400 MHz, $CDCl_3$): δ 0.94 (m, 6H, 2× CH_3), 1.20–1.27 (m, 1H, CH_2), 1.37–1.51 (m, 2H, CH, CH_2), 1.57–1.64 (m, 1H, CH_2), 1.79–1.87 (m, 1H, CH_2), 2.53–2.68 (m, 2H, CH_2), 7.27 (d, 2H, *J* = 8.8, Ar), 7.81 (d, 2H, *J* = 8.5, Ar), 7.98 (m, 4H, Ar). **^{13}C NMR** (100 MHz, $CDCl_3$): δ 11.31 (CH_3), 18.84 (CH_3), 29.13 (CH_2), 31.35 (CH_2), 32.26 (CH_2), 34.03 (CH), 113.96 (CCN), 118.45 (CN), 122.44 (2× CH, Ar), 123.34 (2× CH, Ar), 124.58 (2× CH, Ar), 133.21 (2× CH, Ar), 149.84 (C), 153.72 (C), 154.39 (C), 172.12 (C=O). **IR**: ν̃ 2960, 2929, 2874, 2224, 1767, 1586, 1494, 1460, 1413, 1380, 1340, 1310, 1291, 1226, 1199, 1137, 1094, 1008, 910, 1069, 1012, 926, 847 cm^{-1}. **HRMS** (APCI+): $C_{20}H_{21}N_3O_2$ calcd for $[(M + H)^+]$ 336.17065; found: for $[(M + H)^+]$ 336.17090.

(*S*)-4-[(4-Cyanophenyl)diazenyl]phenyl-2-(hexyloxy)propanoate (Ib)

The material **Ib** was prepared according to the method **B** in 86% (260 mg) yield as orange crystals, m.p. 49–50 °C.

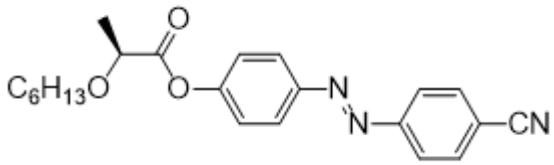

Method **B**. A mixture of an acid (1.2 mmol) with a catalytic amount of DMF (0.05 mL) in oxalyl chloride (10 mL) was stirred at room temperature for 2 h. The excess of oxalyl chloride was distilled from the mixture. The residue was dissolved in hexane (10 mL) and treated with active charcoal at reflux. After the mixture was filtered while hot, hexane was evaporated and the crude acid chloride was mixed with a solution of DMAP (1.1 mmol) and the phenol **1** (1 mmol) in DCM (5 mL). The mixture was stirred in an argon atmosphere at room temperature for 8 h and then decomposed with 17% aq. hydrochloric acid. Layers were separated and the aqueous layer was extracted with toluene (2 × 20 mL). The combined organic solution was washed with brine (10 mL) and dried with anhydrous magnesium sulfate. The solvent was removed, and the crude orange product was purified by column chromatography (eluent: chloroform) and multiple crystallizations from ethanol.

^{1}H NMR (400 MHz, $CDCl_3$): δ 0.89 (m, 3H, CH_3), 1.28–1.43 (m, 6H, 3× CH_2), 1.58–1.69 (m, 5H, CH_2, CH_3), 3.50 (m, 1H, CH_2O), 3.70 (m, 1H, CH_2O), 4.22 (m, 1H, CH), 7.30 (m, 2H, Ar), 7.82 (m, 2H, Ar), 7.99 (m, 4H, Ar). **^{13}C NMR** (100 MHz, $CDCl_3$): δ 14.04 (CH_3), 18.70 (CH_3), 22.60 (CH_2), 25.74 (CH_2), 29.73 (CH_2), 31.63 (CH_2), 70.85 (CH_2O), 74.98 (CH), 114.06 (C̲CN), 118.44 (CN), 122.23 (2× CH, Ar), 123.38 (2× CH, Ar), 124.65 (2× CH, Ar), 133.24 (2× CH, Ar), 150.00 (C), 153.38 (C), 154.35 (C), 171.65 (C=O). **IR**: ṽ 2945, 2929, 2857, 2237, 1719, 1604, 1585, 1503, 1459, 1426, 1400, 1350, 1278, 1213, 1136, 1104 cm^{-1}. **HRMS** (APCI+): $C_{22}H_{25}N_3O_3$ calcd for $[(M + H)^+]$ 380.19687; found: for $[(M + H)^+]$ 380.19692.

(*R*)-4-[(4-Cyanophenyl)diazenyl]phenyl-2-[4-(octyloxy)phenoxy]propanoate (Ic)

The material **Ic** was prepared according to the method **A** in 84% (268 mg) yield as orange crystals, m.p. 87–88 °C.

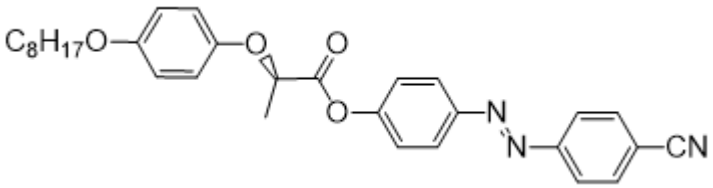

^{1}H NMR (400 MHz, $CDCl_3$): δ 0.88 (t, 3H, *J* = 6.8, CH_3), 1.25–1.48 (m, 10H, 5× CH_2), 1.73–1.80 (m, 5H, CH_2, CH_3), 3.91 (d, 2H, *J* = 6.6, CH_2O), 4.93 (q, 1H, *J* = 6.8, CH), 6.86 (d, 2H, *J* = 9.1, Ar), 6.94 (d, 2H, *J* = 9.1, Ar), 7.22 (d, 2H, *J* = 8.8, Ar), 7.81 (d, 2H, *J* = 8.5, Ar), 7.97 (d, 4H, *J* = 8.6, Ar). **^{13}C NMR** (100 MHz, $CDCl_3$): δ 14.10 (CH_3), 18.62 (CH_3), 22.65 (CH_2), 26.05 (CH_2), 29.23 (CH_2), 29.34 (CH_2), 29.36 (CH_2), 31.80 (CH_2), 68.56 (CH_2O), 73.74 (CH), 114.08 (C̲CN), 115.46 (2× CH, Ar), 116.66 (2× CH, Ar), 118.41 (CN), 122.18 (2× CH, Ar), 123.37 (2× CH, Ar), 124.62 (2× CH, Ar), 133.21 (2× CH, Ar), 150.07 (C), 151.33 (C), 153.12 (C), 154.31 (C), 154.35 (C), 170.68 (C=O). **IR**: ṽ 2953, 2919, 2852, 2230, 1760, 1591, 1512, 1497, 1475, 1457, 1394, 1288, 1228, 1198, 1173, 1152, 1127, 1105, 1050, 1031, 1011 cm^{-1}. **HRMS** (APCI+): $C_{30}H_{33}N_3O_4$ calcd for $[(M + H)^+]$ 500.25438; found: for $[(M + H)^+]$ 500.25500.

(*S*)-4-[(4-Cyanophenyl)diazenyl]phenyl 4-(4-methylhexanoyloxy)benzoate (IIa)

The material **IIa** was prepared according to the method **A** in 88% (135 mg) yield as orange crystals, m.p. 79–80 °C.

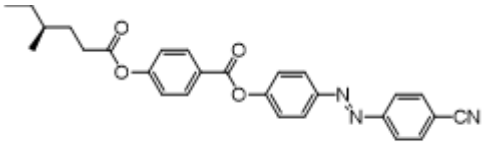

^{1}H NMR (400 MHz, $CDCl_3$): δ 0.94 (m, 6H, 2× CH_3), 1.20–1.27 (m, 1H, CH_2), 1.39–1.49 (m, 2H, CH, CH_2), 1.55–1.64 (m, 1H, CH_2), 1.79–1.88 (m, 1H, CH_2), 2.54–2.68 (m, 2H, CH_2), 7.27 (d, 2H, *J* = 8.6, Ar), 7.41 (d, 2H, *J* = 8.7, Ar), 7.82 (d, 2H, *J* = 8.4, Ar), 8.00 (d, 2H, *J* = 8.4, Ar), 8.05 (d, 2H, *J* = 8.7, Ar), 8.27 (d, 2H, *J* = 8.6, Ar). **^{13}C NMR** (100 MHz, $CDCl_3$): δ 11.31 (CH_3), 18.84 (CH_3), 29.13 (CH_2), 31.32 (CH_2), 32.25 (CH_2), 34.03 (CH), 114.02 (C$\underline{C}$N), 118.45 (CN), 121.99 (2× CH, Ar), 122.59 (2× CH, Ar), 123.38 (2× CH, Ar), 124.68 (2× CH, Ar), 126.73 (C), 131.87 (2× CH, Ar), 133.23 (2× CH, Ar), 150.01 (C), 153.78 (C), 154.38 (C), 155.22 (C), 163.96 (C), 171.91 (C=O). **IR**: ṽ 2960, 2920, 2872, 2225, 1755, 1733, 1597, 1504, 1485, 1412, 1380, 1308, 1291, 1259, 1226, 1198, 1162, 1140, 1115, 1103, 1069, 1012, 926, 850 cm^{-1}. **HRMS** (APCI+): $C_{27}H_{25}N_3O_4$ calcd for [(M + H)$^+$] 456.19178; found: for [(M + H)$^+$] 456.19173.

(*S*)-4-[(4-Cyanophenyl)diazenyl]phenyl-4-{[2-(hexyloxy)propanoyl]oxy}benzoate (IIb)

The material **IIb** was prepared according to the method **A** in 78% (160 mg) yield as orange crystals, m.p. 73–74 °C.

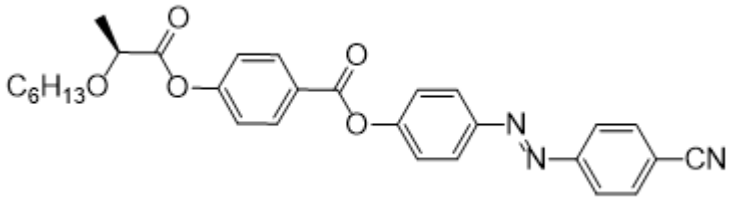

^{1}H NMR (400 MHz, $CDCl_3$): δ 0.86 (t, *J* = 8.0, 3H, CH_3), 1.25–1.52 (m, 11H, 4× CH_2, CH_3), 3.51 (m, 1H, CH_2O), 3.71 (m, 1H, CH_2O), 4.23 (m, 1H, CH), 7.30 (d, 2H, *J* = 8.6, Ar), 7.41 (d, 2H, *J* = 8.7, Ar), 7.82 (d, 2H, *J* = 8.4, Ar), 7.99 (d, 2H, *J* = 8.4, Ar), 8.05 (d, 2H, *J* = 8.7, Ar), 8.27 (d, 2H, *J* = 8.6, Ar). **^{13}C NMR** (100 MHz, $CDCl_3$): δ 14.04 (CH_3), 18.67 (CH_3), 22.56 (CH_2), 25.75 (CH_2), 29.71 (CH_2), 31.61 (CH_2), 70.87 (CH_2O), 74.96 (CH), 114.00 (C$\underline{C}$N), 118.44 (CN), 121.81 (2× CH, Ar), 122.58 (2× CH, Ar), 123.38 (2× CH, Ar), 124.70 (2× CH, Ar), 126.73 (C), 131.95 (C), 133.23 (2× CH, Ar), 150.03 (C), 153.73 (C), 154.37 (C), 154.88 (C), 163.91 (C=O), 171.49 (CH$\underline{C}$=O). **IR**: ṽ 2956, 2931, 2859, 2240, 1766, 1735, 1600, 1504, 1486, 1457, 1412, 1374, 1306, 1275, 1206, 1162, 1127, 1075, 1014, 849, 808 cm^{-1}. **HRMS** (APCI+): $C_{29}H_{29}N_3O_5$ calcd for [(M + H)$^+$] 500.21800; found: for [(M + H)$^+$] 500.21809.

2.3. Experimental on Mesomorphic Behavior and Photoresponse of the Target Materials

Sequence of phases and phase transition temperatures of the **IIa,b** materials were determined by observations of characteristic textures and their changes in polarizing optical microscope (POM) NIKON Elipse E600Pol (Nikon, Tokyo, Japan) and checked by Differential Scanning Calorimetry (DSC) Perkin-Elmer 8000 (Perkin-Elmer, Waltham, MA, USA) on cooling and heating runs at a rate of 5 K min^{-1}. The DSC samples of 3–8 mg were placed in a nitrogen atmosphere and hermetically sealed in aluminum pans. Temperature and enthalpy change values were calibrated on the extrapolated onset temperatures and the enthalpy changes of the melting points of water, indium, and zinc. The study of characteristic textures by observation in POM have been carried out using home-made glass cells with indium-tin oxide (ITO) transparent electrodes (5 × 5 mm^2) and polyimide layers unidirectionally rubbed, which ensured planar-aligned (quasi-bookshelf) geometry. The sample thickness was defined by Mylar sheets as 5 μm. The temperature of the samples was precisely controlled by using Linkam LTS E350 (Linkam, Tadworth, UK) heating/cooling stage with a TMS 93 temperature controller (Linkam, Tadworth, UK); it assures the temperature stability of 0.1 K.

The photoresponse of the materials **IIa,b** in each mesophase was studied using POM on ITO-cells (5 μm thick, planar alignment) filled with the studied materials at temperature several degrees above the clearing point. The designed LC materials were cooled down to a desired temperature and illuminated with UV-light (wavelength 365 nm, intensity 11.3 $mW \cdot cm^{-2}$) using a LED diode source (Height-Led, Shenzhen, China). After reaching the photostationary state, the sample was left to relax.

3. Results and Discussion

3.1. Mesomorphic Properties

Mesomorphic properties of the prepared materials were studied using POM and DSC. Results of these measurements are summarized in Table 1. DSC heating/cooling runs are presented in Figure 3.

Table 1. Sequence of phases, phase transition temperatures (°C) measured on cooling (5 K min^{-1}) and melting points, m.p. (°C), measured on heating (5 K min^{-1}) determined by Differential Scanning Calorimetry (DSC) for the **Ia-c** and **IIa,b** materials.

Material	m.p.	Cr	T_{cr}	M_3	T_{tr}	M_2	T_{tr}	M_1	T_{tr}	Iso
Ia	92.6	•	73.6	–		–		–		•
Ib	49.7	•	−5.9	–		–		–		•
Ic	88.5	•	49.0	–		–		–		•
IIa	81.4	•	46.4	SmA*	99.7	TGBA*	118.1	N*	259.5	•
IIb	81.3	•	55.7	–		SmA*	159.4	N*	175.5	•

m.p.—melting point, °C; Cr—crystalline phase; T_{cr}—crystallization temperature, °C; M1–M3—order of formed mesophases on cooling; T_{tr}—transition temperature, °C; Iso—isotropic liquid state; N*—chiral nematic phase; SmA*—orthogonal smectic A* phase; TGBA*—the frustrated twist grain boundary A* phase; •/–—a phase exists/not exists.

To compare properties of the designed novel materials with those known from the literature (Figure 2), we have summarized their properties in Table 2. In order to provide the full picture for considering the structure–property relationships, and related effects of the diazenyl linking unit and chiral units, the data on chiral cyanobiphenyl-based materials listed as well.

Table 2. Mesomorphic properties of the known materials.

Material	T_{cr}	M_3	T_{tr}	M_2	T_{tr}	M_1	T_{tr}	Iso	Ref.
Non-chiral OCB materials									
6-OCB	57.0	–		–		N	75.7	•	
12-OCB	56.5	–		SmA		–	90.0	•	[21,22,49]
8-COOCB	42.5	–		SmA	63.0	N	76.0	•	
Chiral CB and OCB materials									
$C_2H_5CH(CH_3)C_2H_4$-CB		–		SmA	−19	N *	−8	•	
$C_2H_5CH(CH_3)C_2H_4$-OCB		–		–		N *	21.5	•	[13,24,25]
$H_{17}C_8OPhO$-CH(CH_3)CO-OCB		–		–		N *	−40	•	
Two-cores CAB and OCAB materials									
7-CAB	76	–		–		N	80.0	•	[50]
7-OCAB	91.0	–		–		N	110.0	•	[50]
Three-cores OCAB materials									
9-OC_6H_4-CO-OCAB	94.0	RN	116.0	SmA	212.4	N	242.9	•	[51]
6-OC_6H_4-CO-OCAB	107.5	–		SmA	124.0	N	276	•	[51]
5*-OC_6H_4-CO-OCAB	58.9	–		–		N *	200.1	•	[40]

m.p.—melting point, °C; Cr—crystalline phase; T_{cr}—crystallization temperature, °C; M1–M3—order of formed mesophases at cooling; T_{tr}—transition temperature, °C; Iso—isotropic liquid state; N—nematic phase; SmA—smectic A phase; RN—reentrant nematic phase; *—chiral mesophase; •/–—a phase was/was not observed.

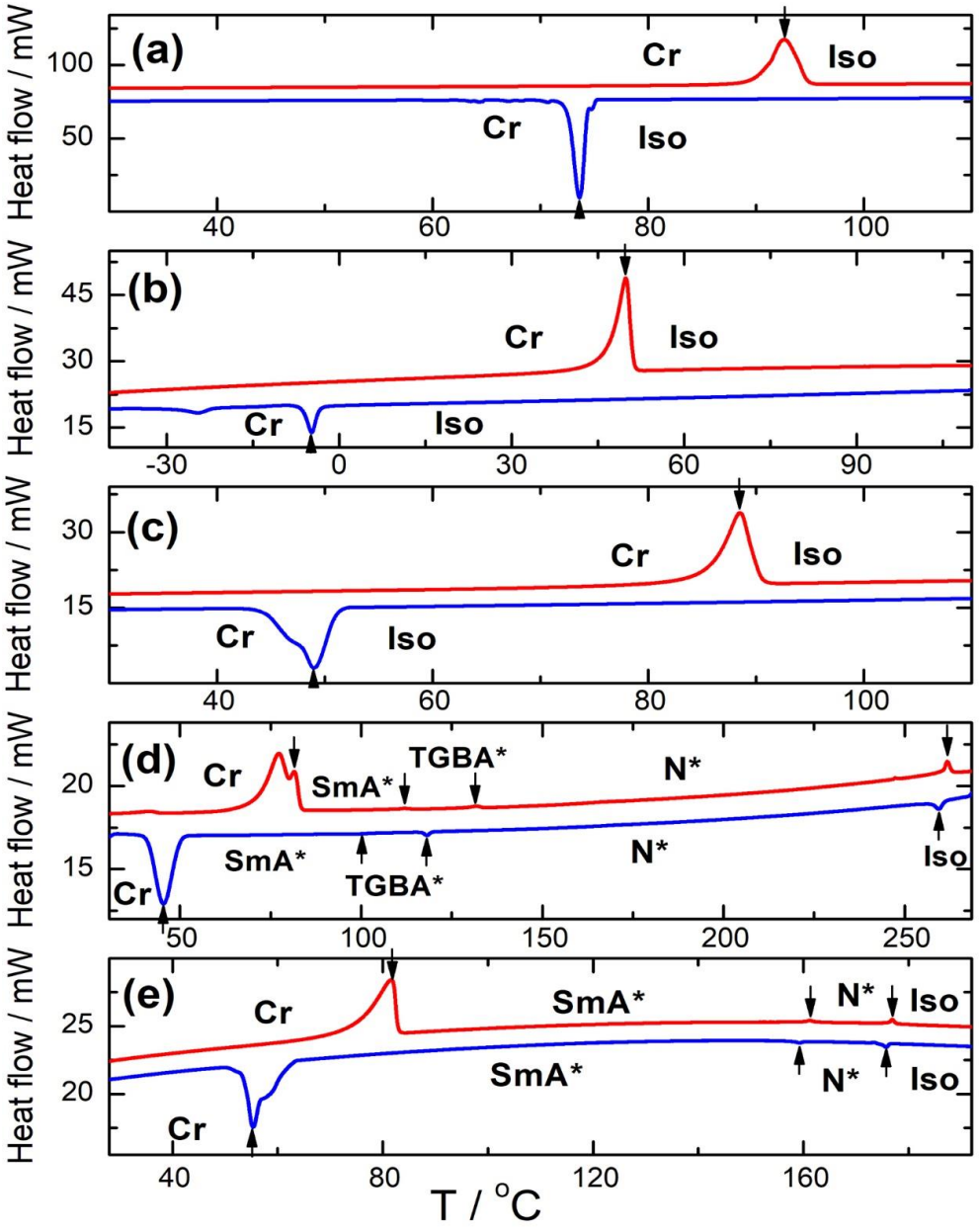

Figure 3. DSC plots of the heating/cooling runs (red/blue curves, respectively) for: **Ia** (**a**), **Ib** (**b**), **Ic** (**c**), **IIa** (**d**), and **IIb** (**e**) materials. Vertical arrows indicate the peaks corresponding to phase transitions; all phases are indicated.

The presented data show that in contrast to known **8-COOCB** and its homologues [51], the material **Ia** is not liquid crystalline. Similarly, the material **Ib** bearing the chiral lactate group was crystalline only. Moreover, the acylated OCB material, namely $\mathbf{H_{17}C_8OPhO\text{-}CH(CH_3)CO\text{-}OCB}$, exhibited a low temperature chiral nematic phase [13], while the material **Ic**, possessing the same molecular structure, except for the diazenyl unit in the central core, was also crystalline. This indicates that the elongation of the biphenyl core by the introduction of the diazenyl spacer into the molecular structure can potentially suppress the formation of mesophases. The introduction of this linker induces a change in the geometry of the central core. Moreover, there is a difference in the ratio between the size of the central core and the length of the connected flexible chain. Both these aspects may play a role in the resulting loss of the mesomorphic behavior.

The extension of the rigid part of the molecule from two to three aromatic cores in materials **IIa,b** was favorable for the formation of mesophases. The material **IIa** exhibited a sequence of three mesophases, namely the TGBA*, SmA*, and N*, in a relatively broad temperature range. The material **IIb** possessing the lactic acid-based chiral center formed two mesophases SmA* and N*. Such behavior is similar to the non-chiral materials **n-OC$_6$H$_4$-CO-OCAB**, which exhibited SmA and N phases, eventually with a re-entrant nematic phase (Table 2). The introduction of the chiral center in the terminal part of the molecule led in case of the material **IIb** to the reduction of transition temperatures and, consequently, to the narrowing of the interval of mesomorphic behavior in comparison with the non-chiral materials. In case of the material **IIa**, the clearing temperature remained similar to the non-chiral material, while the crystallization temperature dropped down resulting in a significant broadening of the interval of the mesomorphic behavior. Furthermore, the compound **IIb** can be directly compared with the material **Ic** that possesses the chiral unit between aromatic cores, which breaks up the system of three interconnected aromatic units. It is obvious that placing the chiral center close to the terminus of the molecule in **IIb** (and **IIa**) is favorable for mesogenicity of the material.

Comparing the properties of **IIa,b** with the chiral representative of the OCAB family (**5*-OC$_6$H$_4$-CO-OCAB**) [40], the materials **IIa,b** form several mesophases. This can be attributed to the elongation of the terminal alkyl chain, which contributes to the stabilization of lamellar order. Additionally, there could be contribution from the ester linkage unit, which was used to connect the chiral terminal unit. This structural feature most probably contributes the stabilization of the lamellar order and the formation of the frustrated mesophase. To the best of our knowledge, material **IIa** is the only representative of the OCAB-family, which exhibits the frustrated TGBA* phase before the crystal phase.

3.2. Photoresponsiveness of the Materials

Since molecules of the liquid crystalline materials **IIa,b** comprise the photoswitchable diazenyl group, their geometry can be modulated using UV-light (365 nm). Light induced changes in geometry (switch from *E*- to *Z*-isomer, Figure 4) result in changes of the supramolecular arrangement. Commonly, a mesophase is isothermally switched to the isotropic state [2] or to a different mesophase under UV-light irradiation [50,52,53]. Crystalline phase, usually, shows no response to UV-light irradiation, relatively few examples of such behavior found in liquid crystals has recently been reviewed [54]. Thus, in this aspect, materials **IIa** and **IIb** showed an unusual response to irradiation.

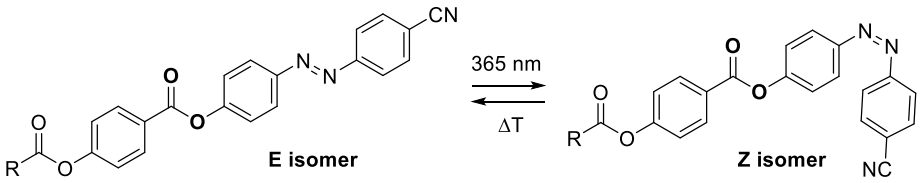

Figure 4. UV-light induced *E*- to *Z*-isomerization of the prepared materials **IIa,b**.

The N* phase of **IIa** showed an ordinary response to irradiation; it was immediately switched to the isotropic phase. The SmA* phase of **IIa**, however, switched first to a remarkably stable N* phase. Up to 4 min of illumination with UV-light was required to force full conversion of the formed N* phase to the Iso phase (Figure 5). The isothermal SmA* → N* phase transition was observed during almost whole temperature range of the SmA* phase existence, which is rather remarkable behavior, since UV light-triggered supercooling in phototropic LCs is usually limited to maximum tens of °C [5,55]. Isothermal relaxation of the UV-light induced Iso phase to the SmA* phase also went through the formation of N* phase. The TGBA* phase has shown an identical behavior.

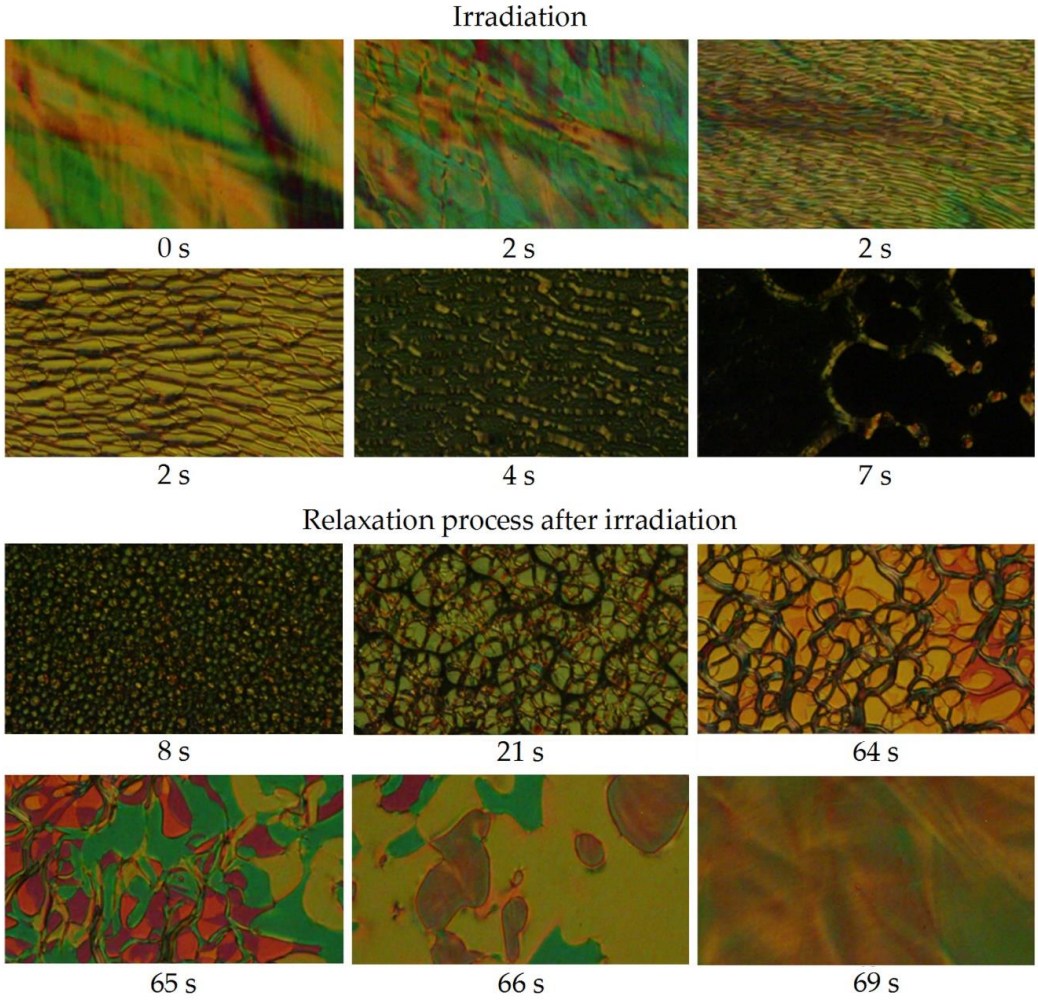

Figure 5. Photos of structural changes in SmA* mesophase of the material **IIa** in a planar ITO-cell at 95 °C observed in POM: before irradiation (0 s); during UV-light (365 nm) irradiation in time (2–7 s) and after irradiation (relaxation process) in time (8–69 s). Initial fast structural changes of the mesophase are assigned with the same time 2 s. The width of each microphotograph is about 250 μm. The whole transition is documented in a supplementary video file Mov_Fig5.

During studies of photoresponse, the **IIa** sample crystallized at 65 °C. Interestingly, UV-light irradiation of this crystalline phase lead to the direct formation of a coexisting mixture of the N* and Iso phases, skipping the SmA* phase (Figure 6). It should be stressed, that isotropic phase was formed at 65 °C instead of 260 °C. The crystalline phase at 60 °C had firstly the same response to UV-light, but during further irradiation crystals grew up in the formed N* + Iso phases mixture, indicating, that at this temperature the crystallization process is already preferred. Below this temperature Cr phase showed no response to the UV-light. Observed Cr → N* + Iso phase transition clearly proves, that this change was not induced by overheating of the material, as the SmA* phase, which should be formed in between Cr and N* phases, was missing. It could be argued that the assumed isotropic phase was in fact homeotropic SmA* phase. We cannot exclude this possibility, although planar cells were used, and we were not able to identify the SmA* phase on repeating the experiment.

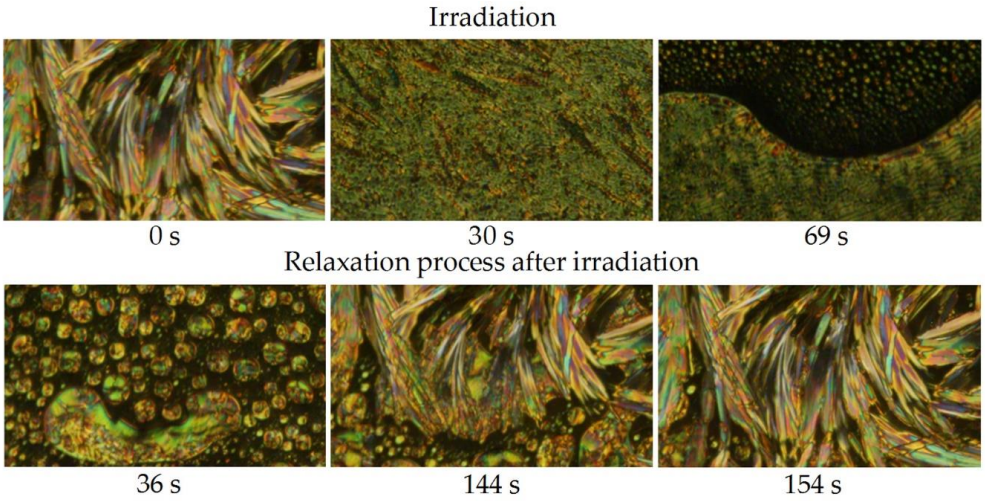

Figure 6. Photos of structural changes in Cr phase of the material **IIa** in a planar ITO-cell at 65 °C observed in POM: before irradiation (0 s); during UV-light (365 nm) irradiation in time (30 s, 69 s) and after irradiation (relaxation process) in time (36–154 s). The whole transition is documented in a supplementary video file Mov_Fig6.

Material **IIb** has also shown an unusual response to UV-light. The N* phase has shown two types of response depending on the temperature of the sample. The common isothermal N* → Iso phase transition induced by illumination with the UV light was observed near the Iso → N* phase transition temperature (around 175 °C). Illumination of the sample at 170 °C induced an N* → N* phase transition. Most probably, the concentration of the UV light induced *Z*-isomer was not high enough to facilitate the transition to isotropic liquid and only a modification of the ordered fluid due to viscosity difference occurred. To clarify this observation, additional measurements providing information on viscosity (e.g., rheological experiment under irradiation) or even the molecular arrangement are required. Irradiation of the SmA* phase close to the phase transition (at 160 °C, measured by POM) resulted in the formation of two N* phases (Figure 7). At 140–135 °C, no UV light-triggered phase transition was observed, but the size of domains changed reversibly (please see the supplementary video file Mov-SI).

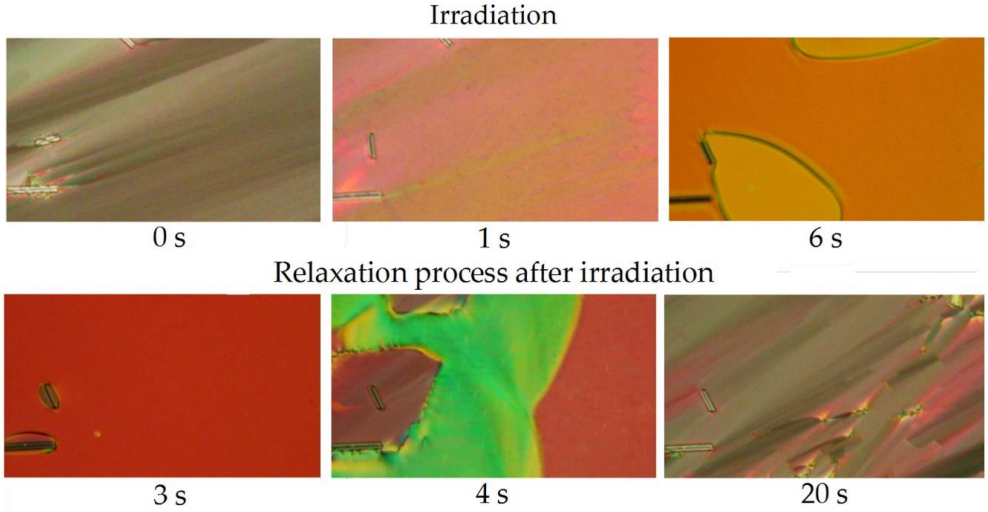

Figure 7. Photos of structural changes in SmA* mesophase of the material **IIb** in a planar ITO-cell at 160 °C observed in POM: before irradiation (0 s); during UV-light (365 nm) irradiation in time (1–6 s) and after irradiation (relaxation process) (3–20 s). The whole transition is documented in a supplementary video file Mov_Fig7.

4. Conclusions

In the current study, we designed two series of novel chiral photosensitive compounds **Ia-c** and **IIa,b**. We have found that only materials **IIa,b** with central core containing three benzene rings and the chiral center located in the terminal part of the molecule possess the liquid crystalline behavior. The materials **IIa,b** exhibited chiral mesophases in a quite broad temperature range up to high temperatures. Both are polymorphic and exhibit chiral smectic and nematic mesophases at low temperatures. To the best of our knowledge, the material **IIa** is the first cyanoazobenzene-based material exhibiting the frustrated TGBA* mesophase.

We have also performed the first study of photoresponse of the monomeric chiral CAB-based materials. We have shown that under irradiation, the N* phase of the material **IIa** is switched to the isotropic liquid. Interestingly, the SmA* and TGBA* phases first switch to a stable N* phase, which on longer irradiation switches to the isotropic phase. Moreover, the crystalline state can be at a certain temperature switched to the coexisting N* and Iso phases. We observed that the N* phase of the material **IIb** at higher temperatures transforms to isotropic liquid and at lower temperatures to a second N* phase. Similarly, the SmA* phase at higher temperatures transforms into two N* phases, while at lower temperatures modulation of the size of its domains has been observed. The obtained results will contribute to better understanding of the molecular structure–mesomorphic property relationship for the liquid crystalline materials possessing the photosensitive moiety as such materials attract considerable attention of the scientific community due to high application potential of those materials for various photonic devices [5,8,56].

Supplementary Materials: The following are available online at https://zenodo.org/record/4317540#.X9yJn9gzZPY, Video S1: Mov_Fig.5, Video S2: Mov_Fig.6, Video S3: Mov-SI, Video S4: Mov_Fig.7.

Author Contributions: Conceptualization, M.K.; methodology, A.P. and M.K.; formal analysis, A.B. and A.P.; investigation, A.B. and A.P.; resources, A.B. and M.K.; writing—original draft preparation, A.P.; writing—review and editing, A.B. and M.K.; project administration, A.B. and M.K.; funding acquisition, A.B. and M.K. All authors have read and agreed to the published version of the manuscript.

Funding: This research was funded by Czech Science Foundation (grant number CSF 19-03564S), Ministry of Education, Youth, and Sports of the Czech Republic (grant number LTC19051), and Operational Programme Research, Development and Education financed by European Structural and Investment Funds and the Czech Ministry of Education, Youth, and Sports (grant number SOLID21—CZ.02.1.01/0.0/0.0/16_019/0000760).

Conflicts of Interest: The authors declare no conflict of interest.

References

1. Brown, G.H.; Shaw, W.G. The Mesomorphic State-Liquid Crystals. *Chem. Rev.* **1957**, *57*, 1049–1157. [CrossRef]
2. Bisoyi, H.K.; Li, Q. Light-Driven Liquid Crystalline Materials: From Photo-Induced Phase Transitions and Property Modulations to Applications. *Chem. Rev.* **2016**, *116*, 15089–15166. [CrossRef] [PubMed]
3. Kawata, S.; Kawata, Y. Three-Dimensional Optical Data Storage Using Photochromic Materials. *Chem. Rev.* **2000**, *100*, 1777–1788. [CrossRef] [PubMed]
4. Asquini, R.; d'Alessandro, A. *Tunable Photonic Devices Based on Liquid Crystals and Composites*; SPIE: Bellingham, WA, USA, 2013; Volume 8828.
5. Jing, H.; Xu, M.; Xiang, Y.; Wang, E.; Liu, D.; Poryvai, A.; Kohout, M.; Éber, N.; Buka, Á. Light Tunable Gratings Based on Flexoelectric Effect in Photoresponsive Bent-Core Nematics. *Adv. Opt. Mater.* **2019**, *7*, 1801790. [CrossRef]
6. Petsch, S.; Rix, R.; Khatri, B.; Schuhladen, S.; Müller, P.; Zentel, R.; Zappe, H. Smart artificial muscle actuators: Liquid crystal elastomers with integrated temperature feedback. *Sens. Actuators A Phys.* **2015**, *231*, 44–51. [CrossRef]
7. Zeng, H.; Wani, O.M.; Wasylczyk, P.; Kaczmarek, R.; Priimagi, A. Self-Regulating Iris Based on Light-Actuated Liquid Crystal Elastomer. *Adv. Mater.* **2017**, *29*, 1701814. [CrossRef] [PubMed]
8. Bobrovsky, A.; Mochalov, K.; Solovyeva, D.; Shibaev, V.; Cigl, M.; Hamplová, V.; Bubnov, A. Laser-induced formation of "craters" and "hills" in azobenzene-containing polymethacrylate films. *Soft Matter* **2020**, *16*, 5398–5405. [CrossRef] [PubMed]

9. Bobrovsky, A.; Shibaev, V.; Cigl, M.; Hamplová, V.; Pociecha, D.; Bubnov, A. Azobenzene-containing LC polymethacrylates highly photosensitive in broad spectral range. *J. Polym. Sci. Part A Polym. Chem.* **2016**, *54*, 2962–2970. [CrossRef]
10. Bubnov, A.; Iwan, A.; Cigl, M.; Boharewicz, B.; Tazbir, I.; Wójcik, K.; Sikora, A.; Hamplová, V. Photosensitive self-assembling materials as functional dopants for organic photovoltaic cells. *RSC Adv.* **2016**, *6*, 11577–11590. [CrossRef]
11. Andrienko, D. Introduction to liquid crystals. *J. Mol. Liq.* **2018**, *267*, 520–541. [CrossRef]
12. Gray, G.W.; Harrison, K.J.; Nash, J.A. New family of nematic liquid crystals for displays. *Electron. Lett.* **1973**, *9*, 130–131. [CrossRef]
13. Booth, C.J.; Gray, G.W.; Toyne, K.J.; Hardy, J. The Synthesis and Transition Temperatures of Novel Low Molar Mass Cholesteric Materials Derived from (R—(4-Hydroxyphenoxy)propanoic Acid. *Mol. Cryst. Liq. Cryst. Sci. Technol. Sect. A Mol. Cryst. Liq. Cryst.* **1992**, *210*, 31–57. [CrossRef]
14. Balachandran, R.; Panov, V.P.; Panarin, Y.P.; Vij, J.K.; Tamba, M.G.; Mehl, G.H.; Song, J.K. Flexoelectric behavior of bimesogenic liquid crystals in the nematic phase–Observation of a new self-assembly pattern at the twist-bend nematic and the nematic interface. *J. Mater. Chem. C* **2014**, *2*, 8179–8184. [CrossRef]
15. Mandle, R.J.; Davis, E.J.; Archbold, C.T.; Cowling, S.J.; Goodby, J.W. Microscopy studies of the nematic NTB phase of 1,11-di-(1″-cyanobiphenyl-4-yl) undecane. *J. Mater. Chem. C* **2014**, *2*, 556–566. [CrossRef]
16. Ahmed, Z.; Welch, C.; Mehl, G.H. The design and investigation of the self-assembly of dimers with two nematic phases. *RSC Adv.* **2015**, *5*, 93513–93521. [CrossRef]
17. Gorecka, E.; Vaupotič, N.; Zep, A.; Pociecha, D.; Yoshioka, J.; Yamamoto, J.; Takezoe, H. A Twist-Bend Nematic (NTB) Phase of Chiral Materials. *Angew. Chem. Int. Ed.* **2015**, *54*, 10155–10159. [CrossRef]
18. Bruce, D.W.; Donnio, B.; Maggs, A.A.; Marsden, J.R. Melt syntheses of some [PtCl2L2] complexes. *Inorg. Chim. Acta* **1991**, *188*, 41–43. [CrossRef]
19. Shabatina, T.I.; Vlasov, A.V.; Vovk, E.V.; Stufkens, D.J.; Sergeev, G.B. Spectroscopic study of low temperature interactions in Sm-mesogenic cyanophenyl co-condensates. *Spectrochim. Acta Part A Mol. Biomol. Spectrosc.* **2000**, *56*, 2539–2543. [CrossRef]
20. Demortière, A.; Buathong, S.; Pichon, B.P.; Panissod, P.; Guillon, D.; Bégin-Colin, S.; Donnio, B. Nematic-like Organization of Magnetic Mesogen-Hybridized Nanoparticles. *Small* **2010**, *6*, 1341–1346. [CrossRef]
21. Qi, H.; Kinkead, B.; Marx, V.M.; Zhang, H.R.; Hegmann, T. Miscibility and Alignment Effects of Mixed Monolayer Cyanobiphenyl Liquid-Crystal-Capped Gold Nanoparticles in Nematic Cyanobiphenyl Liquid Crystal Hosts. *ChemPhysChem* **2009**, *10*, 1211–1218. [CrossRef]
22. Constant, J.; Raynese, E.P. Flow Aligned Viscosities of Cyanobiphenyls. *Mol. Cryst. Liq. Cryst.* **1980**, *62*, 115–123. [CrossRef]
23. Das, M.K.; Paul, S.; Paul, R. X-ray Diffraction Studies on Solid and Mesomorphic Phases of Four Members of Alkoxy-Cyanobiphenyls. *Mol. Cryst. Liq. Cryst. Sci. Technol. Sect A Mol. Cryst. Liq. Cryst.* **1995**, *264*, 89–98. [CrossRef]
24. Gray, G.W.; Kelly, S.M. Mesomorphic Transition Temperatures and Viscosities for Some Cyano-biphenyls and p-terphenyls with Branched Terminal Alkyl Groups. *Mol. Cryst. Liq. Cryst.* **1984**, *104*, 335–345. [CrossRef]
25. Gray, G.W.; McDonnell, D.G. Synthesis and Liquid Crystal Properties of Chiral Alkyl-Cyano-Biphenyls (and -p-Terphenyls) and of Some Related Chiral Compounds Derived from Biphenyl. *Mol. Cryst. Liq. Cryst.* **1976**, *37*, 189–211. [CrossRef]
26. Dunmur, D.A.; Tomes, A.E. Molecular Properties of Pentyl-Cyano Mesogens Having Different Core Structures. *Mol. Cryst. Liq. Cryst.* **1983**, *97*, 241–253. [CrossRef]
27. Eidenschink, R.; Erdmann, D.; Krause, J.; Pohl, L. Substituted Phenylcyclohexanes—A New Class of Liquid-Crystalline Compounds. *Angew. Chem. Int. Ed. Engl.* **1977**, *16*, 100. [CrossRef]
28. Grachev, V.T.; Zaitsev, B.E.; Itskovich, E.M.; Pavluchenko, A.I.; Smirnova, N.I.; Titov, V.V.; Dyumaev, K.M. Spectroscopic and Quantum-Chemical Study of Structure of Liquid Crystalline Cyanobiphenyls and Arylcyanopyridines. *Mol. Cryst. Liq. Cryst.* **1981**, *65*, 133–144. [CrossRef]
29. Brettle, R.; Dunmur, D.A.; Marson, C.M.; Milagros, P.; Kazuhisa, T. New Liquid Crystalline Compounds Based on Thiophene. *Chem. Lett.* **1992**, *21*, 613–616. [CrossRef]
30. Cigl, M.; Bubnov, A.; Kašpar, M.; Hampl, F.; Hamplová, V.; Pacherová, O.; Svoboda, J. Photosensitive chiral self-assembling materials: Significant effects of small lateral substituents. *J. Mater. Chem. C* **2016**, *4*, 5326–5333. [CrossRef]

31. Fearon, J.E.; Gray, G.W.; Ifill, A.D.; Toyne, K.J. The Effect of Lateral Fluorosubstitution on the Liquid Crystalline Properties of some 4-n-Alkyl-, 4-n-Alkoxy- and Related 4-Substituted-4′-cyanobiphenyls. *Mol. Cryst. Liq. Cryst.* **1985**, *124*, 89–103. [CrossRef]
32. Herman, J.; Harmata, P.; Strzeżysz, O.; Czerwiński, M.; Urban, S.; Kula, P. Synthesis and properties of chosen 4-butyl-phenyltolane derivatives–On the influence of core substitution on birefringence, mesomorphic and dielectric properties. *J. Mol. Liq.* **2018**, *267*, 511–519. [CrossRef]
33. Pal, S.K.; Acevedo-Vélez, C.; Hunter, J.T.; Abbott, N.L. Effects of Divalent Ligand Interactions on Surface-Induced Ordering of Liquid Crystals. *Chem. Mater.* **2010**, *22*, 5474–5482. [CrossRef]
34. Węgłowska, D.; Czerwiński, M.; Kula, P.; Mrukiewicz, M.; Mazur, R.; Herman, J. Fast-response halogenated 4-alkyl-4″-cyano-p-terphenyls as dual frequency addressing nematics. *Fluid Phase Equilib.* **2020**, *522*, 112770. [CrossRef]
35. Cox, R.J.; Clecak, N.J. The Preparation of 4-Cyano-4′-Alkyltolans: A New Series of Liquid Crystals. *Mol. Cryst. Liq. Cryst.* **1976**, *37*, 241–248. [CrossRef]
36. Cox, R.J.; Clecak, N.J. The Preparationof 4-Alkyl-4′-Cyanostilbenes: A New Series of Liquid Crystal Compounds. *Mol. Cryst. Liq. Cryst.* **1976**, *37*, 263–267. [CrossRef]
37. Cross, G.J.; Seed, A.J.; Toyne, K.J.; Goodby, J.W.; Hird, M.; Carmen Artal, M. Synthesis, transition temperatures, and optical properties of compounds with simple phenyl units linked by double bond, triple bond, ester or propiolate linkages. *J. Mater. Chem.* **2000**, *10*, 1555–1563. [CrossRef]
38. Gray, G.W.; Mosley, A. Mesomorphic Transition Temperatures for the Homologous Series of 4-n-Alkyl-4′-Cyanotolanes and Other Related Compounds. *Mol. Cryst. Liq. Cryst.* **1976**, *37*, 213–231. [CrossRef]
39. Karamysheva, L.A.; Kovshev, E.I.; Barnik, M.I. Mesomorphism and Dielectric Properties of Phenyl 4 -Alkylbiphenyl-4′ -Carboxylates and Phenyl 4 (4-Alkylphenyl) cyclohexanecarboxylates. *Mol. Cryst. Liq. Cryst.* **1976**, *37*, 29–34. [CrossRef]
40. Kuvshinov, G.V.; Potemkina, O.V.; Kuvshinova, S.A.; Koifman, O.I. Rod-Like Msogens with Three Aromatic Rings and Chiral Terminal Substituent. *Liq. Cryst. Appl.* **2017**, *17*, 43–55. [CrossRef]
41. Socha, J.; Bekárek, V.; Schreiber, J.; Večeřa, M. Reactivity of organic azo-compounds. XII. Correlation of chemical shift of hydroxyl group in NMR spectra of aromatic hydroxyazo compounds with substituent constants. *Collect. Czechoslov. Chem. Commun.* **1970**, *35*, 3551–3556. [CrossRef]
42. Kenyon, J.; Symons, M.C.R. The oxidation of carboxylic acids containing a tertiary carbon atom. Part II. *J. Chem. Soc.* **1953**, 3580–3583. [CrossRef]
43. Loseva, M.; Chernova, N.; Vorflusev, V.; Beresnev, L.; Hiller, R.; Haase, W. Synthesis and Physical Properties of Novel Terphenyl Type Ferroelectric Liquid Crystals. *Mol. Cryst. Liq. Cryst. Sci. Technol. Sect. A Mol. Cryst. Liq. Cryst.* **1995**, *260*, 261–267. [CrossRef]
44. Bajzíková, K.; Kohout, M.; Tarábek, J.; Svoboda, J.; Novotná, V.; Vejpravová, J.; Pociecha, D.; Gorecka, E. All-organic liquid crystalline radicals with a spin unit in the outer position of a bent-core system. *J. Mater. Chem. C* **2016**, *4*, 11540–11547. [CrossRef]
45. Kobayashi, S.; Ishibashi, S. Ferroelectric Liquid Crystals with Chiral Groups on Each Side of the Core. *Mol. Cryst. Liq. Cryst. Sci. Technol. Sect. A Mol. Cryst. Liq. Cryst.* **1992**, *220*, 1–17. [CrossRef]
46. Poryvai, A.; Vojtylová-Jurkovičová, T.; Šmahel, M.; Kolderová, N.; Tomášková, P.; Sýkora, D.; Kohout, M. Determination of Optical Purity of Lactic Acid-Based Chiral Liquid Crystals and Corresponding Building Blocks by Chiral High-Performance Liquid Chromatography and Supercritical Fluid Chromatography. *Molecules* **2019**, *24*, 1099. [CrossRef] [PubMed]
47. Kohout, M.; Bubnov, A.; Šturala, J.; Novotná, V.; Svoboda, J. Effect of alkyl chain length in the terminal ester group on mesomorphic properties of new chiral lactic acid derivatives. *Liq. Cryst.* **2016**, *43*, 1472–1485. [CrossRef]
48. Poryvai, A.; Bubnov, A.; Pociecha, D.; Svoboda, J.; Kohout, M. The effect of the length of terminal n-alkyl carboxylate chain on self-assembling and photosensitive properties of chiral lactic acid derivatives. *J. Mol. Liq.* **2019**, *275*, 829–838. [CrossRef]
49. Kreger, K.; Wolfer, P.; Audorff, H.; Kador, L.; Stingelin-Stutzmann, N.; Smith, P.; Schmidt, H.-W. Stable Holographic Gratings with Small-Molecular Trisazobenzene Derivatives. *J. Am. Chem. Soc.* **2010**, *132*, 509–516. [CrossRef]

50. Delden, R.A.V.; Mecca, T.; Rosini, C.; Feringa, B.L. A Chiroptical Molecular Switch with Distinct Chiral and Photochromic Entities and Its Application in Optical Switching of a Cholesteric Liquid Crystal. *Chem. Eur. J.* **2004**, *10*, 61–70. [CrossRef]
51. Druon, C.; Wacrenier, J.M. A Study of 4 Nonanoate, 4′ Cyanobiphenyl Using Dielectric Relaxation Method. *Mol. Cryst. Liq. Cryst.* **1982**, *88*, 99–108. [CrossRef]
52. Pieraccini, S.; Gottarelli, G.; Labruto, R.; Masiero, S.; Pandoli, O.; Spada, G.P. The Control of the Cholesteric Pitch by Some Azo Photochemical Chiral Switches. *Chem. Eur. J.* **2004**, *10*, 5632–5639. [CrossRef] [PubMed]
53. Pieraccini, S.; Masiero, S.; Spada, G.P.; Gottarelli, G. A new axially-chiral photochemical switch. *Chem. Commun.* **2003**, 598–599. [CrossRef] [PubMed]
54. Xu, W.-C.; Sun, S.; Wu, S. Photoinduced Reversible Solid-to-Liquid Transitions for Photoswitchable Materials. *Angew Chem. Int. Ed.* **2019**, *58*, 9712–9740. [CrossRef] [PubMed]
55. Sobolewska, A.; Bartkiewicz, S.; Mysliwiec, J.; Singer, K.D. Holographic memory devices based on a single-component phototropic liquid crystal. *J. Mater. Chem. C* **2014**, *2*, 1409–1412. [CrossRef]
56. Bobrovsky, A.; Svyakhovskiy, S.; Bogdanov, A.; Shibaev, V.; Cigl, M.; Hamplová, V.; Bubnov, A. Photocontrollable Photonic Crystals Based on Porous Silicon Filled with Photochromic Liquid Crystalline Mixture. *Adv. Opt. Mater.* **2020**, *8*, 2001267. [CrossRef]